

Advanced Scanner Matching using Freeform Source and Lens

Manipulators

Jong-Ho Lim, Kyung Kang, Sung-Man Kim, Samsung Semiconductor (Republic of Korea); Wenjin Shao, Fei Du, Zhengfan Zhang, Zongchang Yu, John Barbuto, Venu Vellanki, Yu Cao, Ronald Goossens, Brion Technologies, Inc. (United States); Seung-Hoon Park, Chris K. Park, Stefan Hunsche, ASML Korea Co., Ltd. (Republic of Korea); Junwei Lu, Brion Technologies Co., Ltd. (China)

Abstract

Proximity matching is a common activity in the wafer fabs^{1,2,3} for purposes such as process transfer, capacity expansion, improved scanner yield and fab productivity. The requirements on matching accuracy also become more and more stringent as CD error budget shrinks with the feature size as technology advances. Various studies have been carried out, using scanner knobs including NA, inner sigma, outer sigma, stage tilt, ellipticity, and dose. In this paper, we present matching results for critical features of a logic device, between an ASML XT:19x0i scanner and an XT:1700i (reference), demonstrating the advantage of freeform illuminator pupil as part of the adjustable knobs to provide additional flexibility. We also present the investigation of a novel method using lens manipulators for proximity matching, effectively injecting scalar wavefront to an XT:19x0i to mimic the behavior of the XT:1700i lens.

Keywords: Scanner matching, PMFC, Pattern Matcher, FlexRay

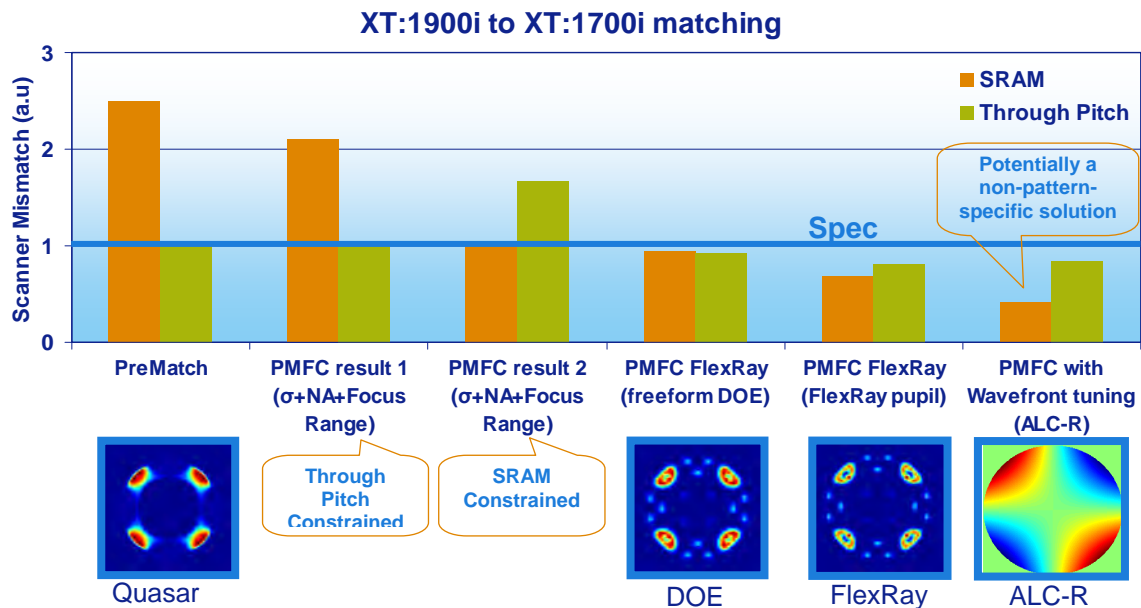


Figure 1: XT:1900i to XT:1700i scanner mismatch. Shown above are simulation results of various matching solutions which were investigated. The data is normalized to the target specification (through-pitch-spec = 1.5 nm and SRAM-spec = 1.0 nm).

Introduction:

Traditional scanner matching methods have been based on 1D proximity matching for a few pitches. However, for 45 nm technology node and below, we need to extend the matching to substantially more pitches. We may also need to include critical device patterns. This can be accomplished with automated tools from ASML such as, Pattern Matcher (PM) and Pattern Matcher FullChip (PMFC). In this paper we demonstrate matching for 45 nm Poly layer considering up to 49 pitches and 3 SRAM CDs using PMFC.

	45nm	32nm	28nm
G-Poly	1.0nm	0.5nm	0.3nm
Patterns	1D+2D	1D+2D	1D+2D

Table 1: Matching requirements by node for poly layer for an advanced logic fab

Pattern type	Stdev for each measurement (nm)	Target Stdev (sigma of mean) (nm)	# repeats required to meet target Stdev
L/S	0.8	0.5	3
2-Bar	0.8	0.5	3
3-Bar	1.6	0.5	11
Line Ends	12.2	1	150
Open T	12.2	1	150
BrickWall	4.1	1	17
Contact	3.3	1	11

Table 2: CD-SEM metrology precision (estimated) for 1D and 2D patterns

Additionally, with each technology node shrink we are seeing the matching specification getting more stringent. An example for matching requirement by node for poly layer is shown in Table 1.

Traditional scanner matching methods use wafer-based CD metrology to characterize the sensitivity of CDs to scanner tuning knobs; this will put extra burden on the already heavy metrology load as the wafer metrology precision on arbitrary 2D patterns is not on par with that of 1D patterns. Typical metrology precision by pattern type using a CD-SEM is shown in Table 2.

As shown in Table 2, to get the required precision for matching at 45 nm node would require a large number of measurement repeats especially for 2D patterns. This metrology burden can be alleviated to a certain degree using computational models for sensitivity and mismatch calculations. In this paper, we explore the possibility of using computational lithography scanner models to drive the scanner matching.

These computational lithography models for scanner matching can be built using CD-SEM data already collected for OPC purposes or can be built using scatterometry-compatible gauges which can be measured with a fast optical metrology tool, such as ASML's YieldStarTM. The scanner-specific model can be built on top of the generic model by using the scanner's in-situ metrology (in the form of a Scanner Fingerprint File) and a few additional measurements collected on a wafer exposed using the specific scanner.

The computational lithography scanner models maximize the use of scanner metrology and design data, thereby reducing the dependence on wafer CD metrology. They also enable calculation of sensitivity to freeform source shapes and to freeform wavefronts which may not be possible using experimental techniques. The models also enable analysis of process window impact due to the various matching solutions. ASML scanner model infrastructure available in LithoTunerTM is very powerful and allows us to explore potential solutions in simulation, with high confidence in accuracy and short turn-around time.

Problem Statement

Most advanced logic fabs, are simultaneously running several dozens of devices. As the loading of these devices could change often, it is most beneficial if all scanners can potentially run all products. In other words, scanner dedication by device is often not an economically feasible solution. Matching in a fab maximizes the flexibility of running products across the available scanner pool. This in turn improves fab capacity and cycle time in addition to CD (thereby yield) performance.

In practice, there is only one OPC process developed using a reference scanner. We need to ensure that transferring an OPC-ed reticle (based on reference scanner) to another scanner will not significantly deteriorate yield. This is accomplished by matching CDs between the scanners. In this paper we used ASML's Pattern Matcher FullChip (PMFC) for accomplishing matching between a reference scanner and a to-be-matched scanner.

In this particular case, we were investigating the transfer of 45nm Poly layer from XT:1700i to XT:1900i. The exposure details are listed below:

- Layer = 4X Poly, NA = 1.2, DOE 13 (quasar), $\sigma_i / \sigma_o = 0.61 / 0.82$
- Patterns: Through Pitch (TP) (49 gauges) and SRAM patterns (3 gauges)
- Reference scanner: XT:1700i, To-be-matched scanner: XT:1900i

The current performance and specification is shown in Table 3.

Maximum CD mismatch →	Target Spec	Current Performance (no tuning)
through-pitch	< 1.5 nm	1.5 nm
SRAM	< 1.0 nm	2.5 nm

Table 3: XT:1900i to XT:1700i matching: Target specification versus current performance as measured on wafer. The numbers indicate maximum (worst) CD mismatch for that pattern category.

Without any scanner tuning the specification for scanner matching is not being met. The reason for the mismatch is mainly driven by the difference in the Jones Pupil of the XT:1700i and XT:1900i lens. For advanced nodes, these aberrations may lead to up to 1-3 nm CD mismatch for some patterns. The scanner mismatch can mainly be captured by swapping the Jones Pupil in the model as shown in Figure 2. PMFC differential calibration³ (diffCal) calibrates the swapped model using the wafer data. This is also

shown in the plot for comparison. As anticipated, PMFC diffCal (blue curve) shows a very good match actual wafer differences (brown curve), however, majority of the difference can be explained by just the swapped model (pink curve).

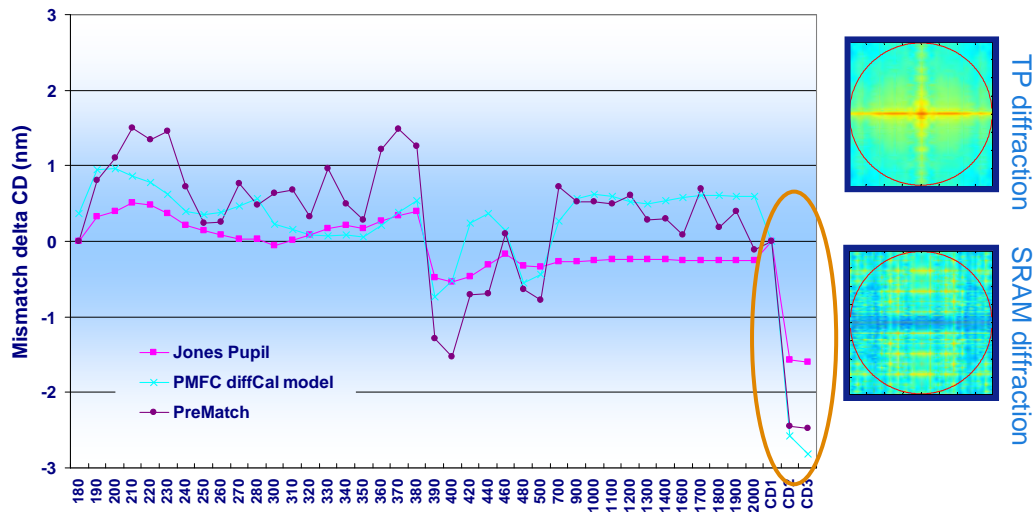


Figure 2: The main source for SRAM mismatch in XT:1900i to XT:1700i is due to differences in Jones Pupil. Different diffraction orders lead to sampling of different parts of the Jones Pupil leading to different amount of mismatch. PreMatch (brown curve) is the measured wafer difference. Jones Pupil (pink curve) is the simulated difference with swapping of the Jones Pupil. PMFC diffCal (blue curve) is the calibrated (based on wafer data and Jones Pupil) scanner mismatch.

Pattern Matcher FullChip (PMFC)

ASML's PMFC uses computational lithography for matching. The objective is to have a to-be-matched scanner print all critical patterns with the same CD as a reference

scanner. This is accomplished by tuning the optical manipulators of the to-be-matched scanner to minimize the CD differences. The manipulators which are currently supported in PMFC include: Numerical Aperture (NA), Partial Coherence (Sigma Inner, Sigma Outer, Ellipticity), Stage Tilt (aka EFSE or Focus Drilling) and exposure Dose.

The optimum manipulator settings depend on the initial CD mismatch and the sensitivity of CD to the manipulators plus any additional constraints on CDs. Scanner-specific models can be used to simulate the initial CD mismatch and the sensitivities. The scanner-specific models are an extension of models used in computational lithography tools such as OPC. This extension is primarily characterized by the reliance on scanner specific on-tool metrology (Scanner Fingerprint File), and by a modified model calibration to account for the sensitivity based approach of scanner tuning.

PMFC tool enables setup of optimization criteria by feature set. The criteria could be in the form of maximum CD mismatch or RMS mismatch constraint. For the XT:1900i to XT:1700i matching case, which was previously discussed, we tried different optimization criteria as shown in the Table 4.

Maximum CD mismatch →	Target Spec	Current Performance (no tuning)	PMFC Constraint: TP < 1.5 nm SRAM < 1nm	PMFC Constraint: TP < 1.5 nm	PMFC Constraint: SRAM < 1nm
through-pitch (TP)	< 1.5 nm	1.5 nm	No solution	1.5 nm	2.5 nm

SRAM	< 1.0 nm	2.5 nm		2.1 nm	1 nm
------	----------	--------	--	--------	------

Table 4: XT:1900i to XT:1700i matching: Target specification versus simulated performance with various PMFC constraints.

As the results indicate, using the available knobs in PMFC we could not find an optimum solution which meets the CD requirements for both through-pitch and SRAM patterns. Furthermore, we see that if we force the maximum CD mismatch criteria on through-pitch, we are out-of-spec on SRAM by 1.1 nm, likewise, if we force the maximum CD mismatch criteria on SRAM, we are out-of-spec on through-pitch by 1 nm. We also, looked into the model prediction accuracy and found that we are able to very well characterize the impact of the knob changes on CDs. An example is shown in Figure 3

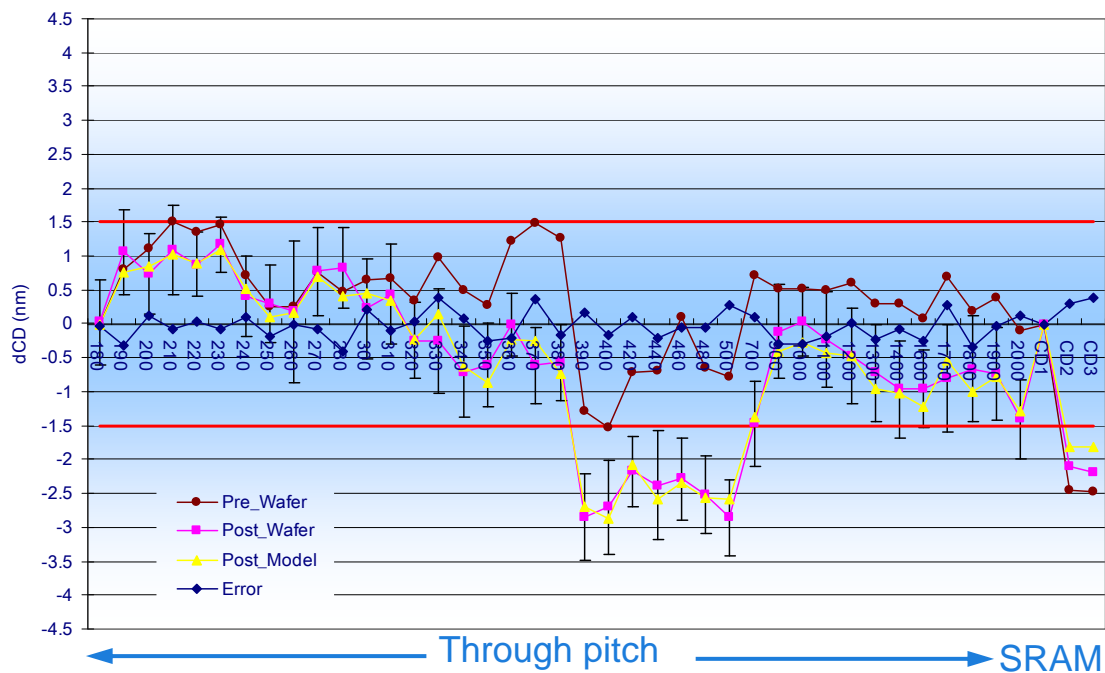


Figure 3: Impact of scanner tuning: The model prediction (yellow) matches wafer measurements (pink) very well.

These results highlight that depending on the gauge sensitivity and initial mismatch a solution which meets a matching requirement may not always be possible with the regular knobs alone. This is highlighted in Figure 4. The plot shows that pre-match CD differences on SRAM is more than Through Pitch (TP). However, sensitivity (to various knobs) of SRAM is small compared to TP patterns. Hence, we have difficulty in meeting spec on both pattern categories.

Using computational tools allows us to find the best compromise for a given set of constraints. To arrive at an optimal compromise using traditional empirical techniques would have taken a long time especially considering the presence of metrology noise.

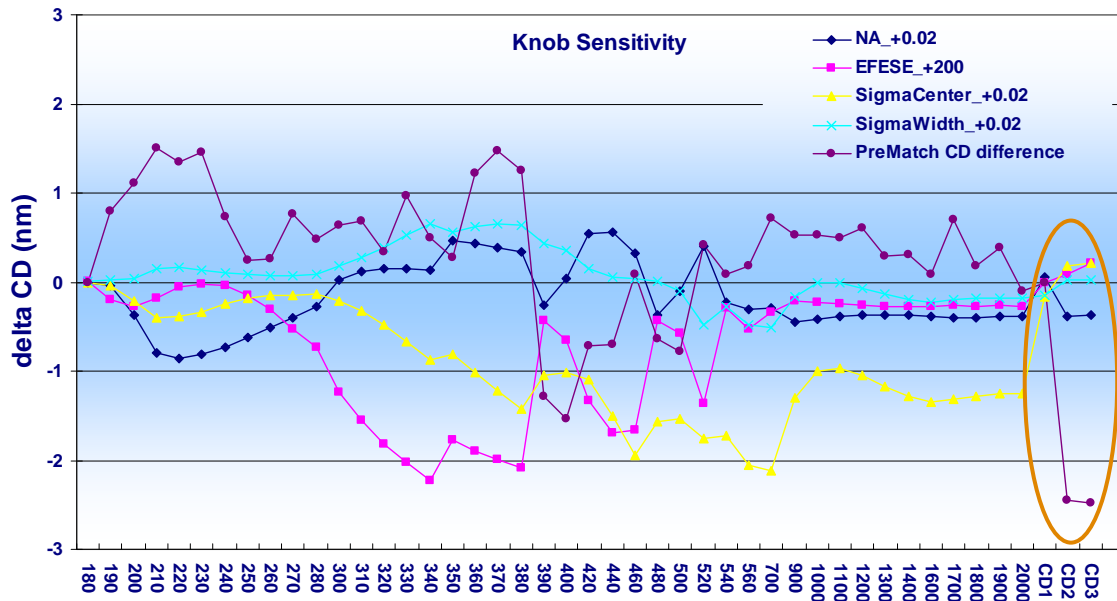


Figure 4: CD change due to scanner “knob” tweak. The numbers indicate pitch values and CD 1-3 indicate SRAM cut-lines.

We looked into the possibility of improving matching further by considering scanner knobs beyond the ones used in PMFC (regular). Three possible knobs were identified:

- Polarized source: We considered using polarization in the source. The reason is that the Jones Pupil difference between the lenses is dominated by polarization-dependant (vector) aberrations. Hence, the source polarization on the XT:1900i could conceivably mimic the polarization-dependant aberration in the XT:1700i

lens. However, polarized source may have different impact on Horizontal versus Vertical patterns, hence, this solution was not pursued.

- Freeform source: A freeform source shape has 100's of degrees of freedom. We have a greater chance of finding an optimum solution which satisfies the matching requirement using a freeform source.
- Lens tuning: We considered adding an aberration to XT:1900i lens using lens manipulator so that it mimics the behavior of the XT:1700i lens. Since, the required lens tuning needed cannot be achieved without the ALC-R lens manipulator, we had to test this functionality on XT:1950i.

In this paper we present the results of using the freeform source and lens tuning.

PMFC FlexRay for Freeform tuning

We used a 'pre-production' version of ASML's PMFC FlexRay product to create an optimal freeform source for improved matching. Freeform source shapes can be rendered in two ways: On AerialXP illuminator using a glass Diffractive Optical Element (DOE) or on FlexRay illuminator using micro-mirror array. There are different constraints for the illuminators mainly driven by spot size, pupil fill ratio and manufacturability. PMFC FlexRay software can find an optimal solution considering all these constraints and output a freeform source which is compatible with the illuminator. In this exercise we only made use of the source shape and did not tune other PMFC knobs. We expect additional benefits when jointly optimizing freeform source shape together with other

PMFC knobs. The simulated matching result using freeform source shapes is shown in Table 5.

Maximum CD mismatch →	Target Spec	Current Perform (measured)	Freeform source with FlexRay (simulated)	Freeform source with glass DOE (simulated)
through-pitch (TP)	< 1.5 nm	1.5 nm	1.2 nm	1.4 nm
SRAM	< 1.0 nm	2.5 nm	0.7 nm	0.9 nm

Table 5: XT:1900i to XT:1700i matching: Target specification versus simulated performance with freeform source.

As noted in Table 5, freeform sources have the capability to meet the matching requirement for 45 nm Poly between XT:1700i and XT:1900i. Unfortunately, the XT:1900i scanner did not yet have the FlexRay upgrade and so we could not do any wafer exposures.

Lens Manipulator tuning

We used an 'engineering' version of ASML's PMFC together with other ASML Tachyon tools to analyze the impact of Lens Manipulators for improved scanner matching.

As a first step, we looked at the Jones Pupil differences together with diffraction map of the critical gauges. We analyzed which aberration has greatest CD sensitivity for the critical gauges and then looked at which aberrations can be easily manipulated with a lens manipulator “knob”. We found that Z6 aberration has a high impact on CD (refer to Figure 5) which is correlated with Jones Pupil and it can also be easily adjusted using the “Advanced Lens Correction – Rotated” (ALC-R) knob. However, any lens element adjustment may sometimes also affect other aberrations – these interdependencies are captured by the Driver Lens Model (DLM). Using this model, we determined that Z6 offset has a parasitic effect on Z5 tilt across the slit. We found through simulation that the amount of Z5 tilt induced by injecting up to 24 nm of Z6 offset did not significantly affect the CDs. Hence, we concluded that we can apply a Z6 offset correction with ALC-R manipulator with confidence that it will not have any additional unexpected impact.

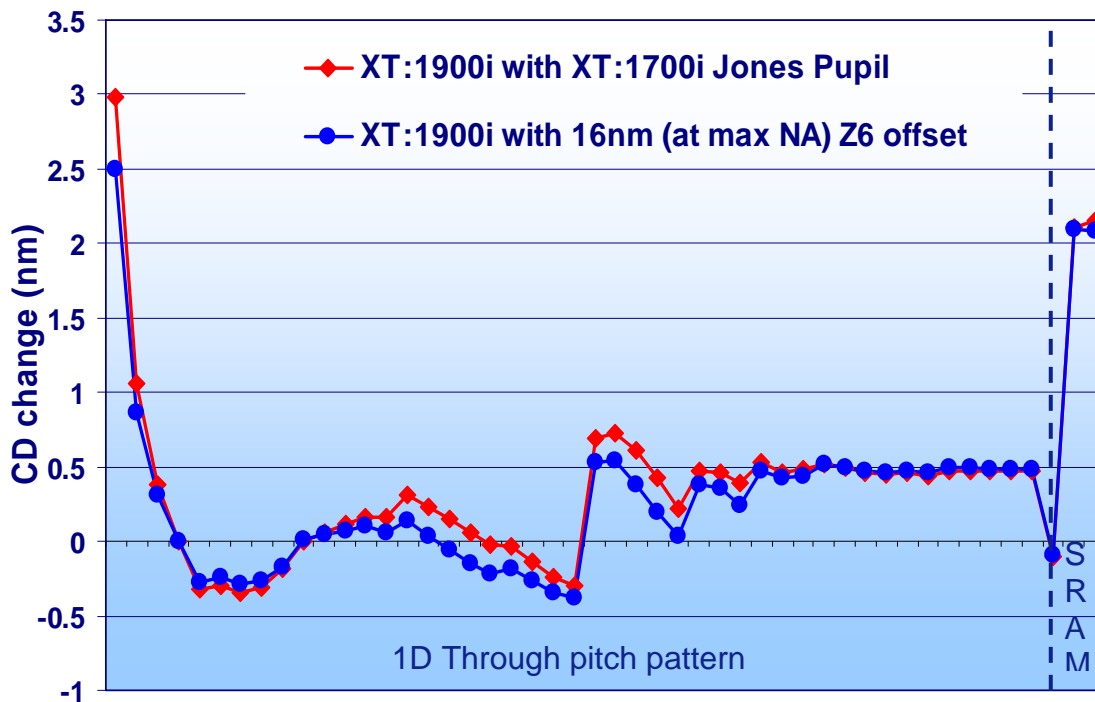


Figure 5: Correlation of CD impact between Jones Pupil of 1700i to Z6 aberration is high.

Z6 aberration which can be manipulated with ALC-R is available as an option on XT:19x0i scanners. Z6 can also be manipulated using the new FlexWaveTM manipulator available on NXT:1950i scanners. Simulation results of applying Z6 tuning is shown in Table 6.

Maximum CD mismatch →	Target Spec	Current Perform (measured)	Z6 tuning (simulated)
through-pitch (TP)	< 1.5 nm	1.5 nm	1.3 nm
SRAM	< 1.0 nm	2.5 nm	0.4 nm

Table 6: XT:1900i to XT:1700i matching: Target specification versus simulated performance with Z6 aberration tuning.

Unfortunately, the ALC-R option was not readily available on XT:1900i to study this. So we instead did wafer exposures on XT:1950i which had the ALC-R option available. We compared the simulated change in CD with Z6 tuning to the wafer measurements and found excellent agreement as shown in Figure 6.

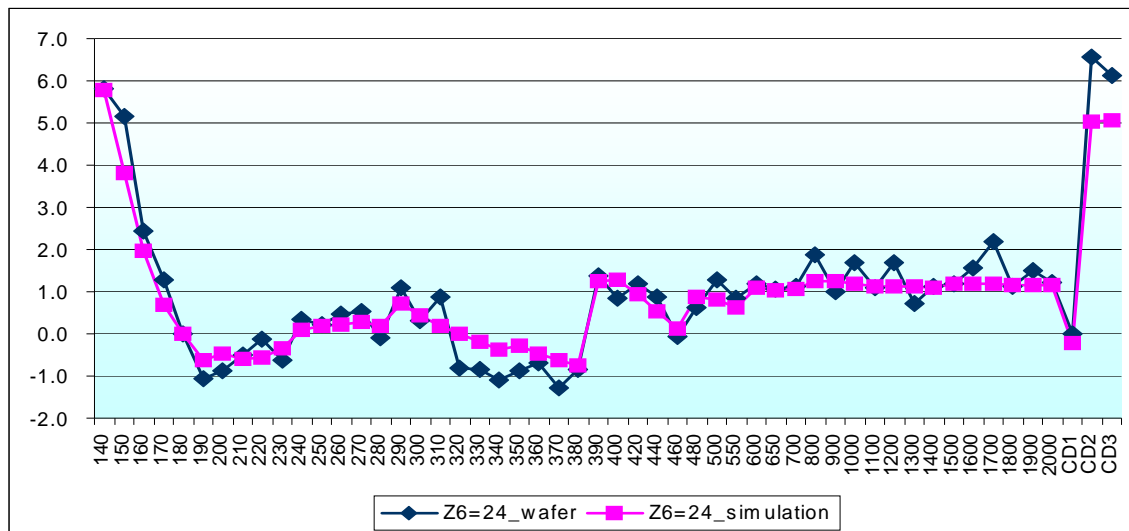


Figure 6: Change in CD due to Z6 tuning is shown. Wafer measurements (on XT:1950i) and simulated results show excellent agreement.

Since, we have wafer results with Z6 tuning only for Z6 = 24 nm, we want to project the change with other Z6 tuning offsets. We know that CD variation with Z6 is quadratic, so we projected CD change for Z6 = 16 nm using the formula: $\Delta CD @ Z6=16 \text{ nm} = \Delta CD @ Z6=24$

$\text{nm} * (16/24)^2$. We then projected the CD change due to Z6 tuning on XT:1900i to XT:1700i mis-match and the results are plotted in Figure 7. The plot indicates best matching performance at Z6 offset of 16 nm. Also, we can see that it meets the matching specification of TP < 1.5 nm and SRAM < 1 nm.

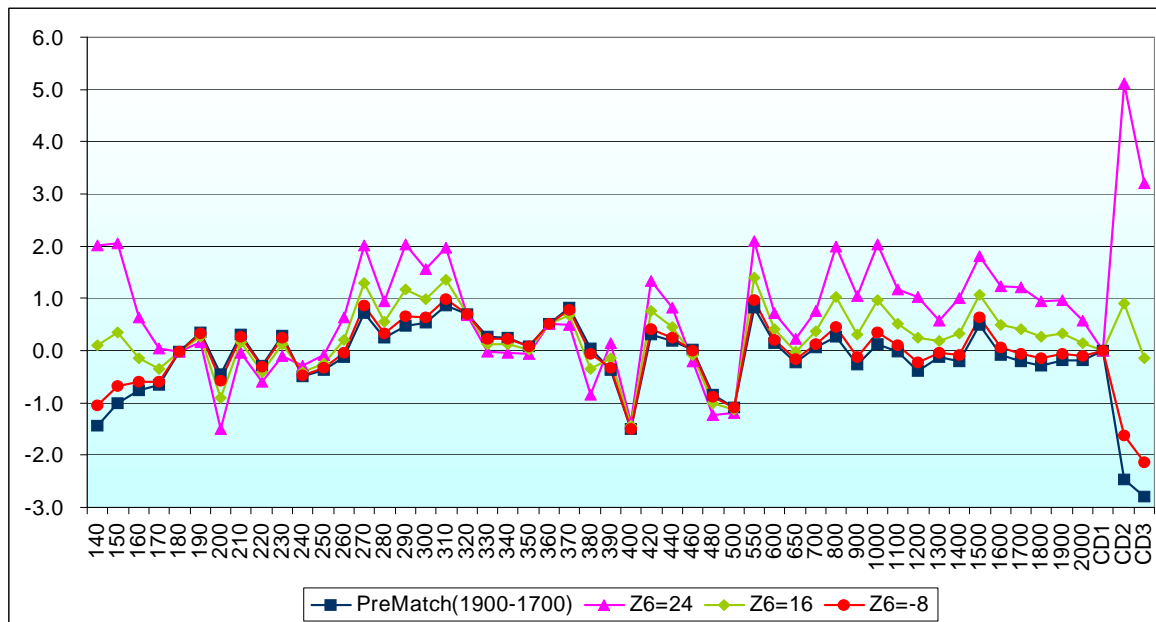


Figure 7: Projected performance of XT:1900i to XT:1700i matching due to Z6 tuning. The projected performance was based on measurement of CD change on XT:1950i due to Z6 tuning. Z6 offset of 16 nm provides best matching performance for XT:1900i to XT:1700i matching.

Jones Pupil with birefringence versus Z6 aberration – Theoretical Study

Using Hopkin's formulation, the Aerial Image CDs for an imaging system can be expressed as a convolution of Transmission Cross Coefficients (TCC) and the Mask.

$$I(x, y) = \sum_{k_{1x}, k_{1y}} \sum_{k_{2x}, k_{2y}} TCC(k_{1x}, k_{1y}; k_{2x}, k_{2y}) M(k_{1x}, k_{1y}) M^*(k_{2x}, k_{2y}) \exp(-i(k_{1x} - k_{2x})x) \exp(-i(k_{1y} - k_{2y})y) \dots (1)$$

Geh et al. demonstrated that Jones pupil can be decomposed into scalar aberration, apodization, birefringence, diattenuation and rotator.⁴ The birefringence in the XT:1700i projection lens contributes the most to the Jones Pupil effect. In this study, we used a hypothetical Jones pupil as a simplification of the actual XT:1700i Jones Pupil. In our hypothetical Jones pupil, we made an assumption about a quadratically increasing radial retardance (aka birefringence) based on the paper of Totzeck et al⁵. In this section, instead of CDs we will compare the TCC due to such a Jones Pupil versus TCC due to Z6 aberration tuning. This facilitates a pattern independent comparison of the effectiveness of using Z6 to compensate for scanner mis-match.

We first prove that when the TCC has C2 symmetry and with thin mask approximation, only the real part of TCC contribute to the aerial image calculation.

For TCC with C2 symmetry,

$$TCC(k_{1x}, k_{1y}; k_{2x}, k_{2y}) = TCC(-k_{1x}, -k_{1y}; -k_{2x}, -k_{2y}) = TCC^*(-k_{2x}, -k_{2y}; -k_{1x}, -k_{1y}) \dots (2)$$

For thin mask, the mask diffraction satisfies the following relation

$$M(k_x, k_y) = M^*(-k_x, -k_y) \dots (3)$$

Substitute (2) and (3) in (1) and rearranging the indices

$$\begin{aligned} I(x, y) &= \sum_{k_{1x}, k_{1y}} \sum_{k_{2x}, k_{2y}} TCC^*(-k_{2x}, -k_{2y}; -k_{1x}, -k_{1y}) M(-k_{2x}, -k_{2y}) M^*(-k_{1x}, -k_{1y}) \exp(-i(-k_{2x} + k_{1x})x) \exp(-i(-k_{2y} + k_{1y})y) \\ &= \sum_{k_{1x}, k_{1y}} \sum_{k_{2x}, k_{2y}} TCC^*(k_{1x}, k_{1y}; k_{2x}, k_{2y}) M(k_{1x}, k_{1y}) M^*(k_{2x}, k_{2y}) \exp(-i(k_{1x} - k_{2x})x) \exp(-i(k_{1y} - k_{2y})y) \dots (4) \end{aligned}$$

Comparing (1) with (4), we see that only the real part of TCC contributes to the aerial image.

Now we demonstrate the similarity between birefringence and Z6 aberration. For an unpolarized source, the TCC can be expressed in terms of the source function (S) and Jones Pupil function (P) as:

$$TCC(k_{1x}, k_{1y}; k_{2x}, k_{2y}) = \sum S(k_x, k_y) [P_{xx}(k_x + k_{1x}, k_y + k_{1y})P_{xx}^*(k_x + k_{2x}, k_y + k_{2y}) + P_{xy}(k_x + k_{1x}, k_y + k_{1y})P_{xy}^*(k_x + k_{2x}, k_y + k_{2y}) + P_{yx}(k_x + k_{1x}, k_y + k_{1y})P_{yx}^*(k_x + k_{2x}, k_y + k_{2y}) + P_{yy}(k_x + k_{1x}, k_y + k_{1y})P_{yy}^*(k_x + k_{2x}, k_y + k_{2y})] \quad \dots(5)$$

A visual comparison of Z6 and a Jones Pupil with birefringence is shown in Figure 8.

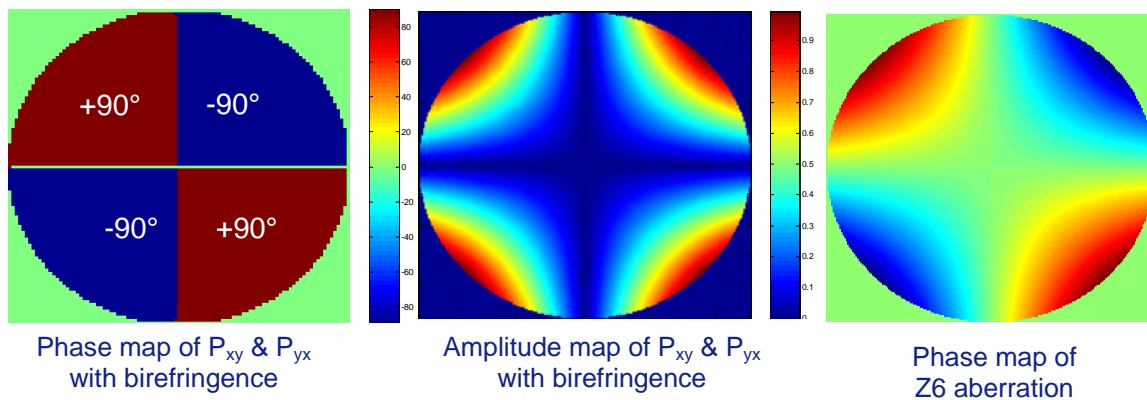


Figure 8 : Visual comparison showing similarity of an ideal Jones Pupil with birefringence versus Z6 aberration.

The Pupil function of the birefringence can be approximated by the equation below:

$$P_{xy}(k_x, k_y) = P_{yx}(k_x, k_y) = ibk_x k_y$$

$$P_{xx}(k_x, k_y) = P_{yy}(k_x, k_y) = \sqrt{1 - b^2(k_x k_y)^2} \cong 1 - \frac{1}{2}b^2(k_x k_y)^2 \quad \dots(6)$$

Where 'b' is a small coefficient which represents the birefringence. Substituting (5) in (6) and ignoring the fourth power of b we get

$$TCC(k_{1x}, k_{1y}; k_{2x}, k_{2y}) = \sum_{kx, ky} S(k_x, k_y) \left\{ 1 - \frac{1}{2} b^2 [(k_x + k_{1x})(k_y + k_{1y}) - (k_x + k_{2x})(k_y + k_{2y})]^2 \right\} \quad \dots(7)$$

The Pupil function in the presence of Z6 coefficient of 'c' can be expressed as:

$$\begin{aligned} P_{xy}(k_x, k_y) &= P_{yx}(k_x, k_y) = 0 \\ P_{xx}(k_x, k_y) &= P_{yy}(k_x, k_y) = e^{ic(k_x k_y)} \end{aligned} \quad \dots(8)$$

Substituting (8) in (5) and only keep the real part of TCC, we get

$$TCC_{real}(k_{1x}, k_{1y}; k_{2x}, k_{2y}) = \sum_{kx, ky} S(k_x, k_y) \left\{ 1 - \frac{1}{2} c^2 [(k_x + k_{1x})(k_y + k_{1y}) - (k_x + k_{2x})(k_y + k_{2y})]^2 \right\} \quad \dots(9)$$

Notice the similarity in (7) and (9). It is clear that an appropriate value for 'c' can be chosen so that it compensates for the birefringence effect 'b' from the Jones Pupil. Hence, a pattern independent compensation can be carried out with Z6 tuning to compensate for Jones Pupil difference between the two scanners.

A full CD simulation was carried out with the actual XT:1700i Jones pupil and the results were previously shown in Figure 5. Hence, the theory matches the simulation and we can say with high confidence that Z6 tuning could be applied for effective compensation of XT:1900i to XT:1700i differences.

Process Window Analysis

Simulation studies on process window impact in using the various tuning solutions were carried out. The results as indicated in Figure 9 show that there is not much Process Window impact due to the Z6 tuning solution. Freeform tuning using DOE and FlexRay has some limited impact on SRAM patterns - there is no exposure latitude (EL) impact but the depth of focus (DoF) decreases by 16% (191 nm → 160 nm).

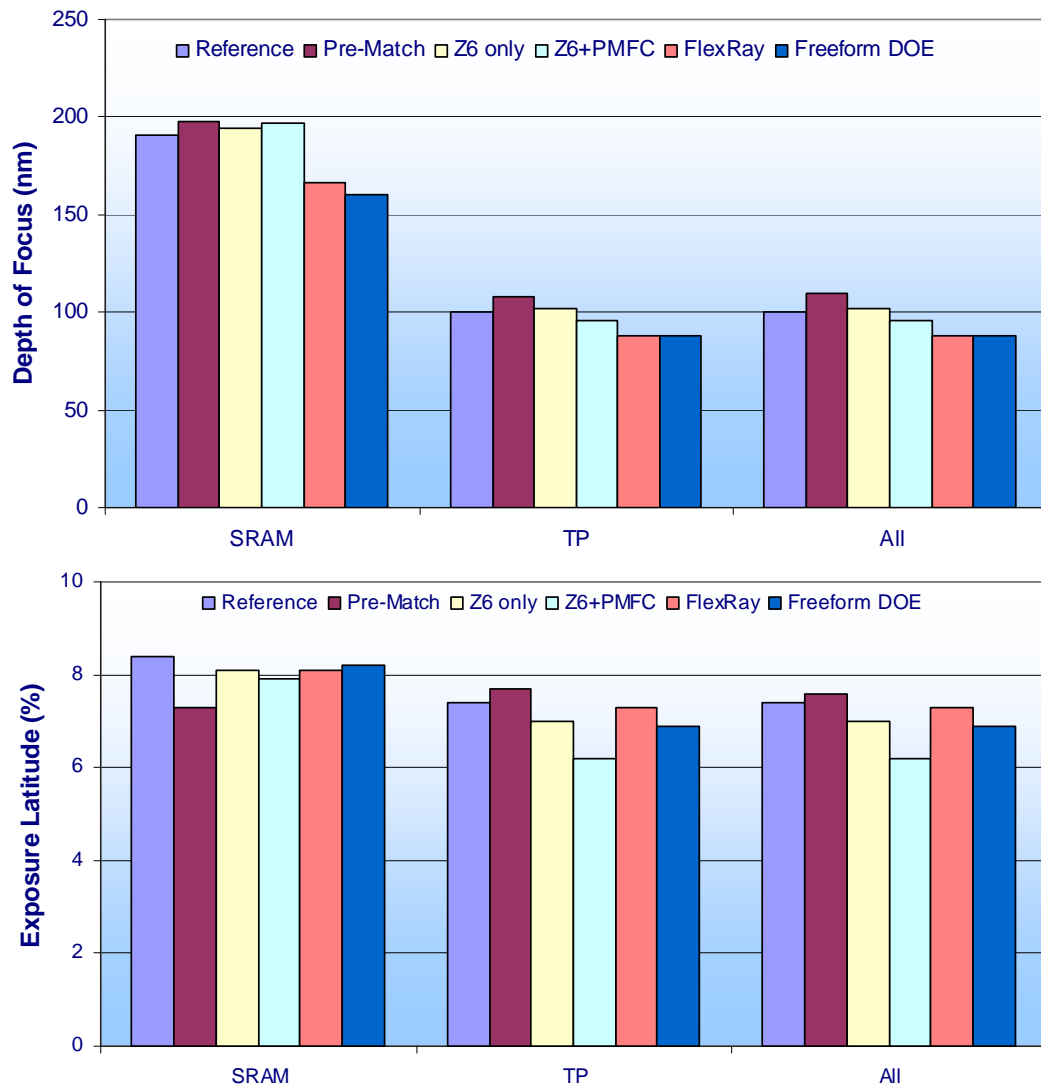


Figure 9: Process Window impact (simulated) due to scanner tuning

Conclusion

In this paper we demonstrated matching of XT:19x0i to XT:1700i using PMFC regular knobs and advanced knobs. For the particular patterns of interest we could not find a

solution which meets the target specification using PMFC tuning with regular manipulators. However, both freeform sources and aberration tuning can be used to meet the matching specification without significantly impacting the process window. We also demonstrated that the LithoTuner model has very good prediction accuracy for regular tuning, freeform tuning and Z6 tuning. Using ASML's PMFC we can quickly tune the scanner pool to obtain optimum matching performance across the critical patterns.

References

- [1] C.Y. Shih et al., "Model-based scanner tuning in a manufacturing environment," Proc. SPIE Vol. 7274, 72740T (2009)
- [2] Yuan He et al., "Simulation-based pattern matching using scanner metrology and design data to reduce reliance on CD metrology," Proc. SPIE Vol. 7640, 764014 (2010)
- [3] Karsten Bubke et al., "Model-based scanner tuning for process optimization," European Mask Lithography Conference (2011)
- [4] Bernd Geh et al., "The impact of projection lens polarization properties on lithographic process at hyper-NA" Proc. Of SPIE Vol. 6520, 65200F (2007)
- [5] Michael Totzeck et al. "Polarization influence on imaging," J. Microlith., Microfab., Microsyst. 4, 031108 (2005)